10.1098/rspa.2003.1126

THE ROYAL SOCIETY

Visco-inertial absorption in dilute suspensions of irregular particles

By S. D. Richards[1], T. G. Leighton[2] and N. R. Brown[2]†

[1]*Marine and Acoustics Centre, QinetiQ, Winfrith Technology Centre, Dorchester DT2 8XJ, UK*

[2]*Institute of Sound and Vibration Research, University of Southampton, Highfield, Southampton SO17 1BJ, UK*

Received 5 September 2002; accepted 20 January 2003; published online 2 July 2003

The presence of mineral particles in suspension results in excess acoustic attenuation which may be significant for high-frequency (tens to hundreds of kilohertz) sonar systems operating in shallow water. Laboratory measurements of absorption at 50–150 kHz in dilute suspensions of spherical, highly non-spherical and natural marine sediment particles are presented and compared with predictions of models for visco-inertial absorption by spherical and spheroidal particles. The methods are validated by the good agreement obtained between the predictions of the spherical model and measurements made with glass spheres. Good agreement is obtained between measurements with plate-like kaolin particles and the predictions of the model for oblate spheroids. Both the spherical and spheroidal models give the approximate magnitude of the attenuation in suspensions of natural marine sediment particles over the frequency range of the measurements.

Keywords: acoustics; ultrasound; absorption; suspension; marine sediment

1. Introduction

The operation of high-frequency (tens to hundreds of kilohertz) sonar systems in shallow, coastal environments is complicated by many phenomena, including rapidly varying bathymetry and sound speed profiles, seabed and sea-surface interactions, tides, currents, turbulence, ambient noise (waves, surf, rain, shipping, marine life) and the effects of bubbles and suspended mineral particles dispersed throughout the water column.

This paper is concerned with the excess acoustic attenuation that arises as a result of the suspended mineral particles that are typically present in shallow, coastal waters. Richards *et al*. (1996) discussed including the effects of suspended particles in high-frequency sonar-performance predictions, using models in which the particles were assumed to be spherical. This work showed that concentrations of the order of 0.1 kg m^{-3} could have a significant impact on high-frequency sonar performance. To test the validity of the spherical models for suspensions of irregular particles, a laboratory measurement technique was developed (Brown *et al*. 1998). This had

† Present address: Industrial Research Limited, PO Box 2225, Auckland 1015, New Zealand.

to be capable of measuring the very small contributions to absorption which dilute suspensions made in a laboratory-scale system.

The aim of the paper is to present the results of measuring absorption in dilute suspensions of spherical and non-spherical particles, and to compare these measurements with predictions based on models for both spherical and spheroidal particles.

2. Theory

Sound propagating in heterogeneous suspensions and emulsions is attenuated by a number of mechanisms in addition to the intrinsic absorption in the constituent components. The sound may be scattered, leading to a loss of energy from the forward-propagating wave, or it may be absorbed through visco-inertial and thermal absorption. Visco-inertial absorption arises when the density of the suspended particles differs from that of the suspending fluid. In this case, the inertia of the particle is not the same as that of the fluid it displaces, and there is a phase lag between the particle and fluid motion. As a result of this, there is a boundary layer at the surface of the particle, in which a velocity gradient exists, leading to damping of the relative motion of the particle by virtue of the fluid viscosity. Thermal absorption results from adiabatic heating and cooling caused by compression and rarefaction in the acoustic field. When the two phases have different thermal diffusivities there is a net transfer of energy from the acoustic field to heat.

A number of modelling approaches have been adopted for computing the coefficients of absorption and scattering in suspensions. Urick (1948) derived the visco-inertial absorption coefficient using simple energy balancing arguments, based on the viscous drag on an oscillating sphere (Stokes 1851). Temkin & Dobbins (1966) discuss a coupled-phase theory, and this has been extended by Evans (1996) to include the effects of particle shape by employing an effective-radius approach. Qian (1996) has presented a modified scattering model which treats suspensions as fractal media, with the Reynolds number as the fractal dimension, and this has been shown experimentally to give good agreement with measured data for various airborne suspensions of irregular particles (Wang *et al*. 2000). However, it is noted that this approach requires that the fractal dimension characterizing the suspension be determined by fitting the model to the observations at a given frequency.

The most complete model for spherical particles is that of Allegra & Hawley (1972), who extended the earlier work of Epstein & Carhart (1953) to include a solid, elastic dispersed phase. The ECAH (Epstein–Carhart–Allegra–Hawley) model yields the total attenuation due to scattering, visco-inertial absorption and thermal absorption by thermally conducting, viscous or elastic spheres suspended in a thermally conducting, viscous fluid.

The ECAH model has the advantage of implicitly including all of the important loss mechanisms. However, its complexity has the effect of obscuring physical insight. Furthermore, its numerical solution is challenging due to problems of ill-conditioning and the large, complex arguments associated with Bessel and Hankel functions and their first and second derivatives. The extension of this model to include the effects of particle shape is impractical.

The current investigation considers suspensions of mineral particles suspended in water, insonified at frequencies of interest to high-frequency sonar systems. This permits two important simplifications. First, there is a large contrast between the

density of the two phases (more than a factor of two), which has the effect that the thermal-absorption term is negligible compared with the visco-inertial term. Second, the wavelengths are large compared with the particle size. Even at 1 MHz, which is in excess of practical sonar frequencies, the acoustic wavelength is *ca.* 1.5 mm, i.e. larger than the particles which are likely to remain in suspension. In this paper, the highest measurement frequency is 150 kHz, corresponding to a wavelength in water of *ca.* 1 cm. This permits long-wavelength approximations to be used for the scattering, i.e. Rayleigh scattering. In fact, in all but the most extreme case of the highest frequency considered (1 MHz) and the largest particles remaining in suspension (of the order of 100 μm), visco-inertial absorption is by far the dominant absorption mechanism. The remainder of this paper is restricted to the analysis of visco-inertial absorption, although it should be noted that, when this work is applied to problems of sonar performance prediction (Richards *et al.* 1996; Richards & Leighton 2000) and monitoring of suspended sediment load in rivers (Richards & Leighton 2001), the scattering term is also included.

Urick (1948) obtained the following expression for the visco-inertial attenuation coefficient by employing the expression for the viscous drag on an oscillating sphere developed by Stokes (1851),

$$\alpha_{\mathrm{v}} = \frac{\phi k(\sigma-1)^2}{2}\left[\frac{s}{s^2+(\sigma+\tau)^2}\right], \tag{2.1}$$

where

$$\tau = \frac{1}{2} + \frac{9}{4}\left(\frac{\delta_{\mathrm{v}}}{a}\right) \tag{2.2}$$

and

$$s = \frac{9}{4}\left(\frac{\delta_{\mathrm{v}}}{a}\right)\left(1+\frac{\delta_{\mathrm{v}}}{a}\right). \tag{2.3}$$

Here ϕ is the volume fraction of suspended particles, k is the acoustic wavenumber, σ is the ratio of the densities of the solid and fluid phases, a is the particle radius and $\delta_{\mathrm{v}} = \sqrt{2\nu/\omega}$ is the skin depth for shear waves, where ν is the kinematic viscosity of the fluid and ω is the acoustic frequency.

Implicit in equation (2.1) is the assumption that the absorption coefficient in a suspension of similar particles is linearly proportional to the volume fraction, ϕ, i.e. the process is linearly additive. This assumption is valid for dilute suspensions, in which inter-particle interactions may be neglected. Urick (1948) showed experimentally that this linear relationship between the viscous absorption coefficient and concentration holds for volume fractions of up to 8–9% for kaolin particles at MHz frequencies. Note that a volume fraction of 8% corresponds to a mass concentration of *ca.* 200 kg m^{-3} for kaolin particles. This is far higher than concentrations found in the natural environment, except perhaps in the boundary region near the seabed.

Equation (2.1) may be extended to account for spheroidal particles by employing expressions for τ and s (Ahuja & Hendee 1978),

$$\tau = L_{\mathrm{i}} + \frac{9}{4}\left(\frac{\delta_{\mathrm{v}}}{b'}\right)K_{\mathrm{sf}}^2 \tag{2.4}$$

and

$$s = \frac{9}{4}\left(\frac{\delta_{\mathrm{v}}}{b'}\right)K_{\mathrm{sf}}^2\left[1 + \left(\frac{1}{K_{\mathrm{sf}}}\right)\left(\frac{\delta_{\mathrm{v}}}{a'}\right)\right], \tag{2.5}$$

where L_{i} is an inertia factor, K_{sf} is a shape factor and a' and b' are, respectively, the semi-major and semi-minor axes for oblate spheroids and the semi-minor and semi-major axes for prolate spheroids. In the case of spheres $L_{\mathrm{i}} = 1/2$, $K_{\mathrm{sf}} = 1$, $a' = b' = a$ and equations (2.4) and (2.5) reduce to equations (2.2) and (2.3), respectively.

The kaolin particles described in § 4 *c* are plate-like in form, and these particles may therefore be represented as oblate spheroids, the degenerate form of which is a circular disc. The inertia coefficient for oblate spheroids oscillating parallel to their axis of symmetry is given by (Lamb 1945)

$$L_{\mathrm{ob},\parallel} = \frac{\alpha_0}{2 - \alpha_0}, \tag{2.6}$$

where

$$\alpha_0 = \left(\frac{2}{\varepsilon^2}\right)\left[1 - \sqrt{1-\varepsilon^2}\left(\frac{\sin^{-1}\varepsilon}{\varepsilon}\right)\right], \tag{2.7}$$

with the eccentricity ε given by

$$\varepsilon = \sqrt{1 - \frac{b'^2}{a'^2}}. \tag{2.8}$$

For oblate spheroids oscillating perpendicularly to their axis of symmetry, the inertia coefficient is

$$L_{\mathrm{ob},\perp} = \frac{\gamma_0}{2 - \gamma_0}, \tag{2.9}$$

where

$$\gamma_0 = \frac{\sqrt{1-\varepsilon^2}}{\varepsilon^3}\sin^{-1}\varepsilon - \left[\frac{1-\varepsilon^2}{\varepsilon^2}\right]. \tag{2.10}$$

The shape factor for oblate spheroids with $h = b'/a' < 1$, for motion parallel to the axis of symmetry, is given by (Happel & Brenner 1965)

$$K_{\mathrm{ob},\parallel} = \frac{8}{3}\left\{\frac{2h}{1-h^2} + \frac{2(1-2h^2)}{(1-h^2)^{3/2}}\tan^{-1}\left[\frac{(1-h^2)^{1/2}}{h}\right]\right\}^{-1}, \tag{2.11}$$

and the shape factor for motion perpendicular to the axis of symmetry is

$$K_{\mathrm{ob},\perp} = \frac{8}{3}\left\{-\frac{h}{1-h^2} - \frac{2h^2-3}{(1-h^2)^{3/2}}\sin^{-1}(1-h^2)^{1/2}\right\}^{-1}. \tag{2.12}$$

3. Experiment

Urick (1948) measured acoustic absorption in suspensions in the MHz frequency range using a pulse-reflection technique. For the frequency range in question, however, no experimental data exist. This reflects the difficulty of taking measurements of the absorption due to dilute suspensions when this is very much less than the absorption due to the boundaries and instrumentation. Previous experimental studies in

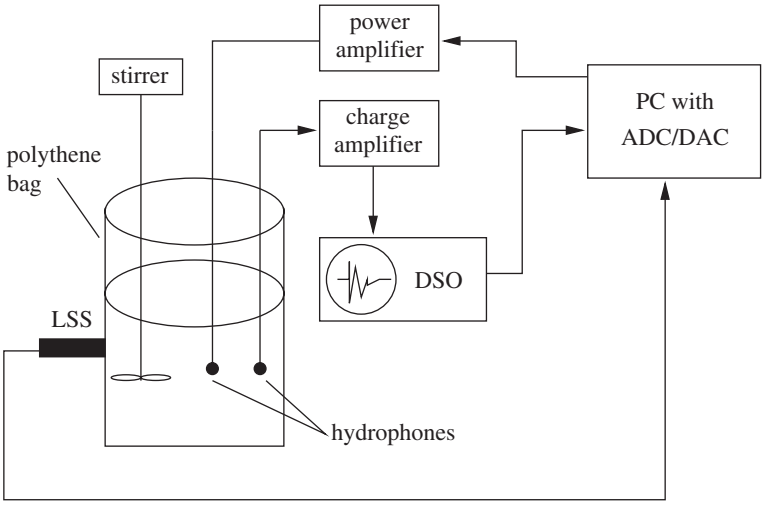

Figure 1. Schematic of the experimental apparatus used to measure absorption in dilute suspensions over 50–150 kHz. The stirrer is removed during acoustic measurements. LSS, light-scattering sensor; ADC/DAC, analog-to-digital and digital-to-analog convertor; DSO, digital storage oscilloscope; PC, personal computer.

aqueous suspensions (e.g. Holmes *et al*. 1994) have employed higher frequencies and volume fractions than those under investigation in this paper. Hence, we have developed a reverberation-time method for measuring absorption in dilute suspensions over the frequency range 50–150 kHz (Brown *et al*. 1998). The use of reverberation-time measurements to determine the attenuation in fluids has been credited by Kurtze & Tamm (1953) to the work of Meyer & Skudrzyk. More recently, the use of reverberation-time measurements to characterize aerosols has been published by Moss & Attenborough (1996). However, application of the reverberation-time technique to examine aqueous suspensions, as in this paper, is complicated by the potential for greater losses at the walls (where the acoustic impedance mismatch is far less than that for airborne suspensions). To overcome this, the sample (which comprises 16 l of deionized and degassed water) is contained within a thin-walled (30 μm) polythene bag, suspended in air by supporting wires, as shown in figure 1 (Brown *et al*. 1997). This arrangement minimizes transmission and absorption at the boundaries by approximating the ideal case of a pressure-release boundary condition. A light-scattering sensor (LSS), mounted horizontally in close contact with the transparent walls of the bag, is used to ensure that the concentration of particles in suspension does not change significantly during the course of the acoustic measurements. A mechanical stirrer is used to re-suspend settled particles prior to the measurements and this is removed while the measurements are made.

A personal computer (PC) equipped with an analog-to-digital and digital-to-analog convertor (ADC/DAC) card generates a 20 ms burst of pseudo-random noise, which is transmitted to the test volume via an amplifier driving a Brüel & Kjaer (B&K) 8103 hydrophone. The aim is to establish a diffuse sound field in the test volume, i.e. one in which the average energy density is the same everywhere and all directions of propagation are equally probable. The lowest frequency at which the sound field may be considered diffuse is given by the Schroeder cut-off frequency (Pierce

1994), which was determined to be *ca.* 50–75 kHz for the test volume described, depending on the reverberation time of the volume. To examine whether an ideally diffuse sound field was achieved, measurements of reverberation time were made with the hydrophones in different positions. This revealed a 4% standard deviation in the reverberation time as a result of the spatial structure in the sound field, and this was found to be the dominant contribution to the overall experimental error (Leighton *et al.* 2002). A second B&K 8103 measures the decaying sound field and the signal is amplified and captured by a digital storage oscilloscope (DSO). The data are transferred to the PC, where they are processed using the method of integrated impulse response (Schroeder 1965) to determine the decay rate of the sound-pressure level. This decay rate is used to find the reverberation time of the volume, i.e. the time taken for the sound-pressure level to decay by 60 dB after the source is switched off.

Each series of measurements begins with the measurement of the reverberation time of the clear water. Carefully weighed quantities of particles are added in stages and measurements are made of the reverberation time of the volume. The additional attenuation due to the particles is inferred from the change in reverberation time of the volume using standard theory for the reverberation time of enclosures (Brown *et al.* 1998).

Further experimental details, including a calculation to show that the turbulence caused by the stirring results in a negligible contribution to the absorption, can be found in Brown *et al.* (1998).

The measurement of low ultrasonic attenuation in very dilute suspensions in a laboratory-scale system was found to be experimentally challenging. The attenuation due to the particles is a very small contribution to the total attenuation in the system, compared with the losses due to the boundaries or the hydrophones themselves. For example, it was observed that a small increase in the hydrophone depth (of the order of millimetres) produced a large increase in the volume attenuation by virtue of the absorption due to the additional length of submerged hydrophone cable (Leighton *et al.* 2002). This effect could be sufficient to obscure the effect of the suspended particles, and care was therefore taken to ensure that the hydrophone positions were kept fixed.

4. Results

(*a*) *Particle characterization*

Absorption measurements are presented for four different particle types: spherical glass beads; kaolin; calcium carbonate; and natural marine sediment particles. Figure 2 shows the measured particle-size distributions, plotted as the percentage of particles by mass whose diameters exceed a particular value, for samples of each of these. In the case of the glass spheres, the particle-size distribution was determined by laser-diffraction analysis. For the other, non-spherical, particulates, three standard particle-sizing techniques were used: laser diffraction; gravitational sedimentation; and centrifugal sedimentation. The samples were exposed to prolonged ultrasound prior to sizing, in an attempt to break up aggregates and ensure that the size distribution of the constituent particles was obtained. The distributions obtained by these methods showed significant differences (Richards 2002), owing to the nature of the measurements: the laser-diffraction method yields the effective sphere diameter for optical scattering, while the sedimentation techniques yield the

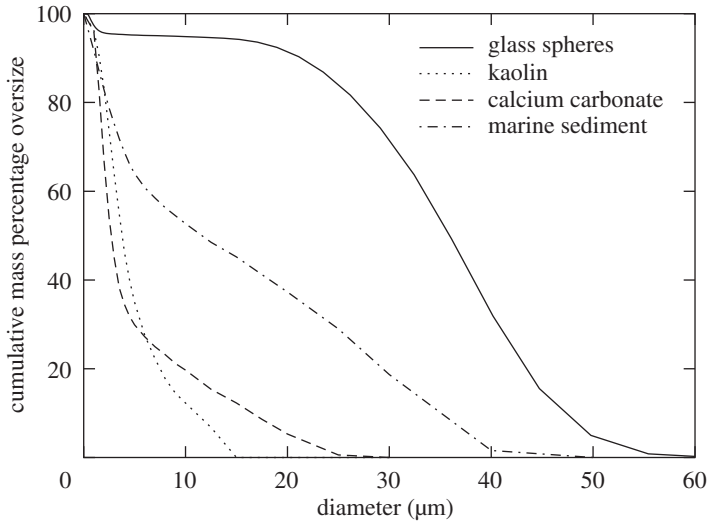

Figure 2. Measured particle-size distributions for the particles under investigation, plotted as the percentage of particles by mass having diameters greater than a given value. The result for glass spheres was determined from laser-diffraction measurements, while the other results are Stokes diameters obtained by gravitational sedimentation.

Stokes diameter, i.e. the diameter of a homogeneous sphere having the same density and settling velocity as the particles under investigation. These differences highlight a fundamental issue in characterizing suspensions of irregular particles and this will be discussed in a future paper. In the current study it was appropriate to use the gravitational-sedimentation result, because both settling under gravity and visco-inertial absorption are characterized by Stokes law. The particle size distributions are taken into account in the theoretical predictions by summing the contributions from each particle-size bin.

(*b*) *Spherical particles*

Initial experiments were performed with homogeneous glass particles. These particles had a high degree of sphericity, enabling direct comparison with the theory for absorption in dilute suspensions of homogeneous spheres.

Figure 3 shows some examples of results for the glass spheres. Measured attenuation data obtained with three different concentrations, normalized with respect to concentration, are plotted against frequency. The data have been processed to yield results at integer multiples of 10 kHz, but the data plotted have been offset slightly in frequency in order that the individual error bars may be resolved. Also shown is the predicted attenuation obtained by integrating equation (2.1) (using equations (2.2) and (2.3)) over the measured particle size distribution shown in figure 2.

While some spread in the data is evident, this figure shows that the majority of the data are in agreement with theory to within experimental error. This gives confidence in the experimental arrangement for measuring attenuation in dilute suspensions over 50–150 kHz.

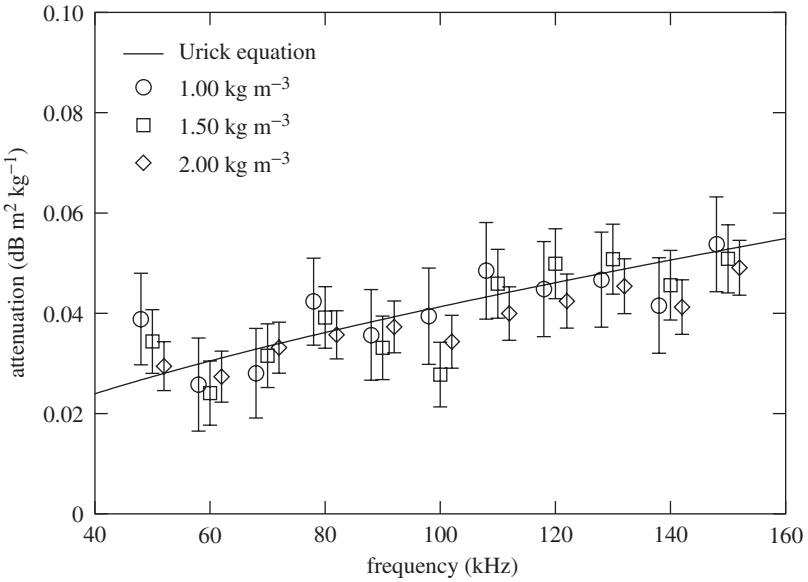

Figure 3. The normalized attenuation coefficient for spherical particles: experimental data and theoretical predictions using Urick's equation. The data points have offsets in frequency as described in the text.

(*c*) *Non-spherical particles*

The preceding section demonstrated the degree of agreement between measurements of absorption made with spherical particles and the Urick model for viscous absorption by spherical particles. The next stage in the experimental programme was to make measurements with non-spherical particles to assess the applicability of the spherical models as the particles depart from sphericity.

For this purpose, two samples of particulates were obtained from ECCI (English China Clays International, now Imerys). The first was a type of kaolin (china clay) with the trade name Speswhite, and the second was a form of calcium carbonate with the trade name Polcarb. Both of these samples were relatively pure and relatively well characterized industrial samples, allowing the study of absorption by non-spherical particles without the problems associated with using natural marine sediments of unknown composition and physical parameters. The Speswhite particles have a density of *ca.* 2600 kg m^{-3}, while the density of the Polcarb is *ca.* 2700 kg m^{-3}. Figure 4 shows an SEM image of a sample of the Speswhite particles and figure 5 shows an image of the Polcarb particles, both imaged at an instrument magnification of $\times$10 000. The Speswhite particles are clearly very plate-like in form, while the Polcarb particles are angular and irregular.

In order to apply the theory for spheroids to these particles it was necessary to determine a representative size distribution of spheroids, rather than the equivalent Stokes diameters, d_{s}, obtained by sedimentation. To achieve this, the settling velocity v_{s} was computed for each particle-size bin in the distribution using

$$v_{\mathrm{s}} = \frac{(\sigma - 1) g d_{\mathrm{s}}^2}{18\nu}, \tag{4.1}$$

where g is the acceleration due to gravity.

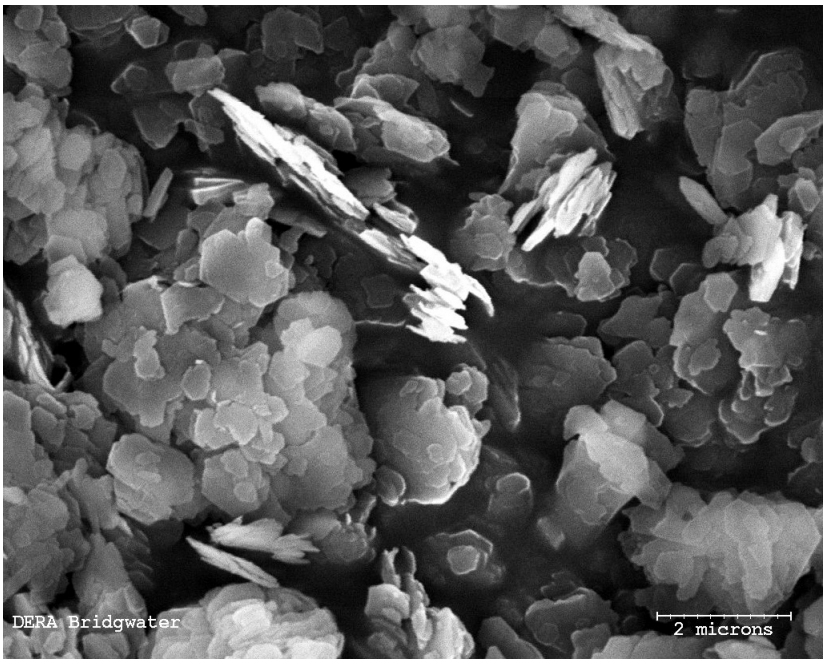

Figure 4. Scanning electron microscope (SEM) image of Speswhite (kaolin) particles using an original instrument magnification of $\times 10\,000$.

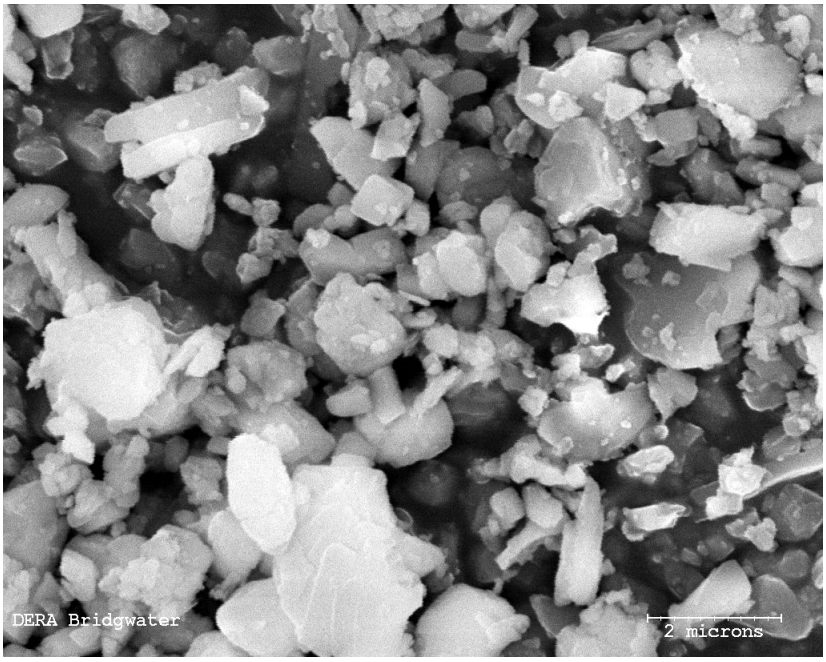

Figure 5. SEM image of Polcarb (calcium carbonate) particles using an original instrument magnification of $\times 10\,000$.

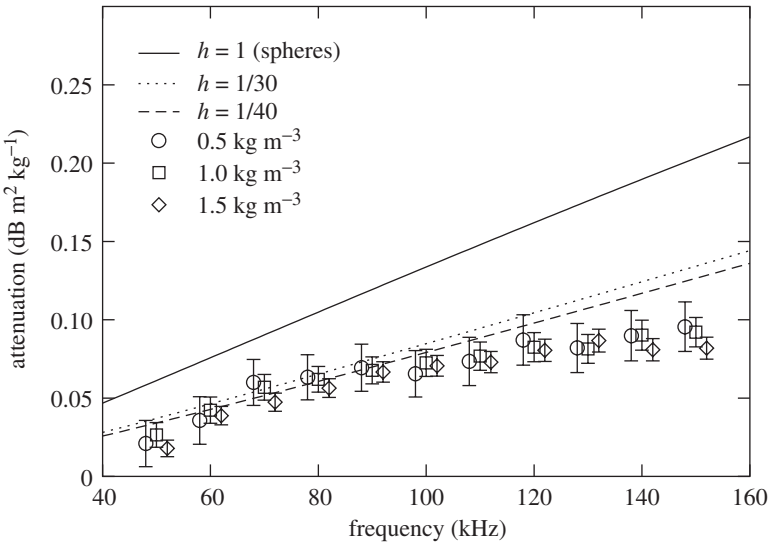

Figure 6. The normalized attenuation coefficient for Speswhite particles: experimental data and theoretical predictions using the model for spheroidal particles. The data points have been offset in frequency as in figure 3.

From this set of settling velocities, the major radii of oblate spheroids with the same set of settling velocities were determined. The Stokes drag force on an oblate spheroid of major radius a' and shape factor K_{sf} settling at velocity v_{s} in a fluid with molecular viscosity η is given by

$$F_0 = 6\pi\eta K_{\mathrm{sf}} a' v_{\mathrm{s}}. \tag{4.2}$$

Equating this to the gravitational/buoyancy force on the spheroid and rearranging to give a' as a function of v_{s} yields

$$a'^2 = \frac{18\nu K_{\mathrm{sf}} v_{\mathrm{s}}}{4h(\sigma - 1)g}. \tag{4.3}$$

The aspect ratio h for the Speswhite particles was stated by the suppliers to be $\frac{1}{30}$–$\frac{1}{40}$. It was assumed that the particles are randomly orientated with respect to the gravitational field and, in the absence of shape factors for arbitrary orientation, it was necessary to average over the two orthogonal orientations. The three independent spatial axes may be resolved into the broadside direction and the two perpendicular edgewise directions for an oblate spheroid. The size distribution was therefore computed assuming two-thirds of the particles to be orientated parallel to the field and one-third to be perpendicular to the field. This is not an important limitation, as the differences between the shape factors for the orthogonal cases were not large.

Figure 6 shows results of measuring the attenuation in suspensions of Speswhite particles, measured at different concentrations and normalized with respect to concentration. The figure also shows the predicted attenuation using equations (2.1), (2.4) and (2.5), assuming $h = 1$ (spheres), $\frac{1}{30}$ and $\frac{1}{40}$. It was assumed that the particles were randomly orientated with respect to the acoustic field, which is a good approximation, since the field is nearly diffuse. This was again approximated by

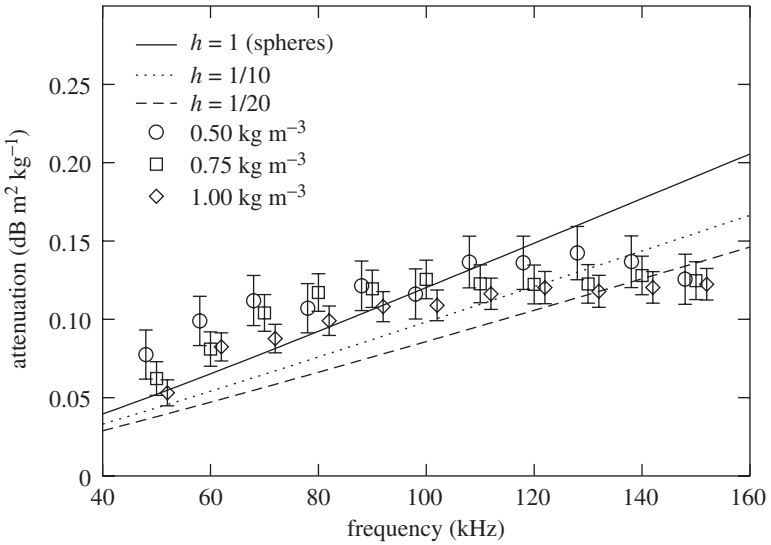

Figure 7. The normalized attenuation coefficient for Polcarb particles: experimental data and theoretical predictions using the model for spheroidal particles. The data points have been offset in frequency as in figure 3.

modelling one-third of the particles in the broadside orientation and two-thirds in the edgewise orientation.

This figure shows that the spherical model significantly overestimates the attenuation due to these flat particles, and this is not surprising given their small aspect ratio. However, the predictions obtained using the aspect ratios quoted by the suppliers show significantly better agreement with the measurements. It is important to note that this agreement was obtained without assuming any *a priori* information about the measurements when modelling the attenuation. It is noted, however, that the predicted frequency dependence differs from the frequency dependence observed in the data.

Figure 7 shows the equivalent result for the Polcarb particles. In this case no aspect ratio data were available and predictions for $h = 1$, $\frac{1}{10}$ and $\frac{1}{20}$ were chosen as they bound the values giving the best agreement with the measurements. Clearly, the agreement between the predictions and measurements is much less good in the Polcarb case than it was in the Speswhite case. This is to be expected, since the plate-like Speswhite particles are approximated well by oblate spheroids, whereas the angular Polcarb particles are not. In this case, the spheroidal model cannot be said to perform any better than the spherical model. Neither model predicts the form of the frequency dependence well, but both give results of a similar magnitude to that obtained by measurement over the frequency range covered.

(*d*) *Natural marine particles*

The measurements with spherical particles described in § 4 *b* enabled the models to be tested in the idealized case. Moving to the Speswhite and Polcarb particles allowed investigations to be carried out with highly non-spherical particles in a relatively controlled way. The final part of the experimental study involved the use of

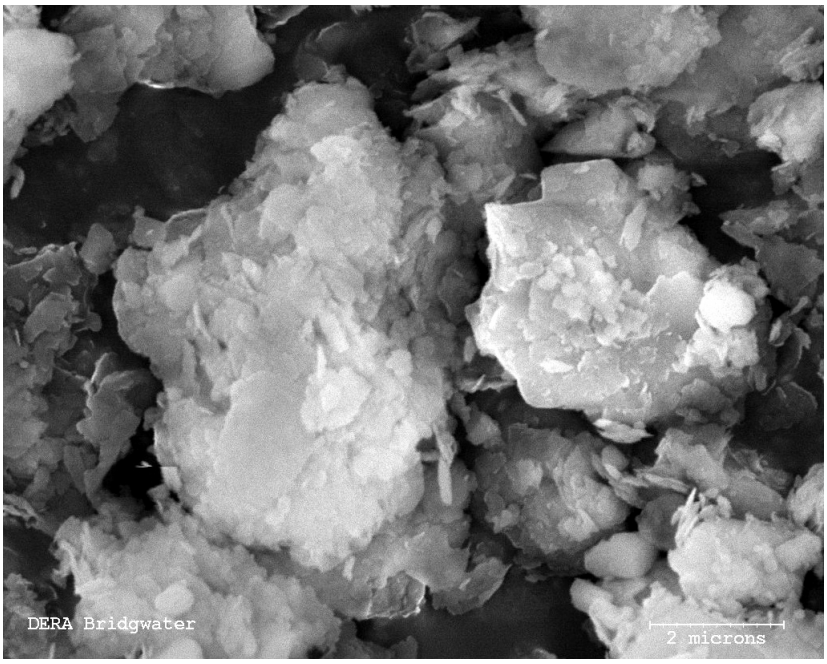

Figure 8. SEM image of marine sediment particles using an original instrument magnification of ×10 000.

real marine-sediment particles from a seabed-sediment core sample. This core was obtained in *ca.* 1600 m of water on the continental slope, west of the Malin Shelf (west of Scotland) and comprises primarily soft grey clay.

Figure 8 shows an SEM image of a typical sample of these sediment particles, imaged at an instrument magnification of ×10 000. This figure, together with other similar examples, shows that the particles are highly irregular and highly variable, with a mixture of plate-like particles and more angular particles. This sample does appear to have similarities with the Speswhite sample, indicating that the sediment contains a significant component of clay-like particles. However, there also appear to be other types of particle present. Although the SEM was not used to identify grain mineralogy, it is likely that the sample will comprise quartz, chlorite, calcite, feldspar and illite (S. G. Healy 2001, personal communication).

Figure 9 shows the result of measuring and modelling the attenuation in dilute suspensions of these marine particles. There is a noticeably larger spread in the data in this figure than was apparent in the previous cases. This may be attributed to the fact that the particles were taken from a wet seabed core sample. The water content was estimated by weighing, drying and re-weighing samples of the core, but spatial variations in water content within the core led to some uncertainty in the dry mass of particles added to the test volume. The mean density of the particles was 2920 kg m^{-3}. It is noted that the data measured at the highest concentration (1.23 kg m^{-3}) appear to be systematically higher than those measured at the lower concentrations. It is further noted that three of the data points for the highest concentration (at 50, 60 and 70 kHz) lie more than one standard deviation above the predictions for spheres.

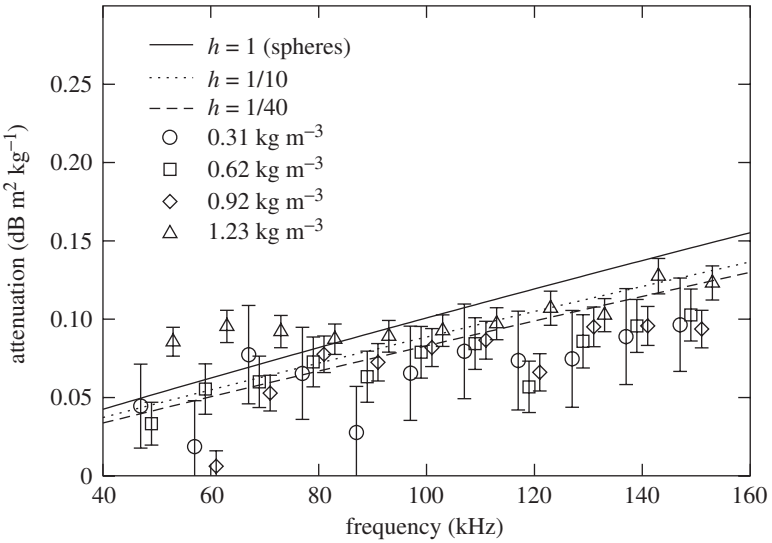

Figure 9. Normalized attenuation coefficient for marine sediment particles: experimental data and theoretical predictions using the model for spheroidal particles. The data points have been offset in frequency as in figure 3.

No aspect ratio data were available for these particles and predictions are shown for $h = 1$, $\frac{1}{10}$ and $\frac{1}{40}$, spanning the range from spheres to the flattest of the kaolin particles. It is difficult to determine whether the spheroidal model yields significantly better agreement with the measurements in this case. Because the sample is characterized by many different particle shapes randomly orientated with respect to the acoustic field, there is an ensemble averaging effect. This means that the spherical model shows reasonable agreement with the measurements, even though the individual particles may not be spherical. Ideally, samples containing a range of particle shapes should be modelled using a distribution of aspect ratios as well as particle sizes, but the data were not available to support this approach in this case. Finally, it is interesting to consider the case of the highest concentration data, in the frequency range 50–70 kHz, which are systematically higher than the predictions for spheres. While the spheroidal model can give an attenuation greater than that for an equivalent distribution of spheres if the spheroids are preferentially orientated edgewise to the flow, this is not the case for the expected averaging over orientation under the conditions of a diffuse acoustic field.

5. Concluding remarks

Laboratory measurements of absorption in dilute suspensions of spherical particles, pure samples of non-spherical particles and natural marine sediment particles have been presented. These measurements have been compared with predictions based on spherical and spheroidal particles. The measurements made with spheres agreed very well with the predictions of the spherical model, which gives confidence in the measurement technique. Predictions of the spheroidal model, using independently determined values for aspect ratio and size distribution, showed good agreement with measurement made with plate-like kaolin particles. The spheroidal model did

not perform significantly better than the spherical model in the case of angular calcium carbonate particles, as expected from the nature of these particles. Reasonable agreement was obtained between measurements made with natural marine sediment particles and both the spherical and spheroidal models. It is expected that the results from the spheroidal model could be improved using a representative distribution of aspect ratios, and the relative success of the spherical model is attributed to ensemble averaging over particle size, shape and orientation.

T.G.L. thanks The Royal Society and the Leverhulme Trust for a Senior Research Fellowship. This work was carried out as part of Technology Group 01 of the MoD Corporate Research Programme and is published with the permission of the Controller of Her Majesty's Stationery Office.

References

Ahuja, A. S. & Hendee, W. R. 1978 Effects of particle shape and orientation on propagation of sound in suspensions. *J. Acoust. Soc. Am.* **63**, 1074–1080.

Allegra, J. R. & Hawley, S. A. 1972 Attenuation of sound in suspensions and emulsions: theory and experiments. *J. Acoust. Soc. Am.* **51**, 1545–1563.

Brown, N. R., Leighton, T. G., Richards, S. D. & Heathershaw, A. D. 1997 Sound absorption by suspended particulate matter. In *Proc. NATO SACLANTCEN Conf. on High Frequency Acoustics in Shallow Water* (ed. N. G. Pace, E. Pouliquen, O. Bergem & A. P. Lyons), pp. 75–82. La Spezia, Italy: NATO SACLANT Undersea Research Centre.

Brown, N. R., Leighton, T. G. & Richards, S. D. 1998 Measurement of viscous sound absorption at 50–150 kHz in a model turbid environment. *J. Acoust. Soc. Am.* **104**, 2114–2120.

Epstein, P. S. & Carhart, R. R. 1953 The absorption of sound in suspensions and emulsions. I. Water fog in air. *J. Acoust. Soc. Am.* **25**, 553–565.

Evans, J. M. 1996 Models for sound propagation in suspensions and emulsions. PhD thesis, The Open University, Milton Keynes, UK.

Happel, J. & Brenner, H. 1965 *Low Reynolds number hydrodynamics*. Englewood Cliffs, NJ: Prentice Hall.

Holmes, A. K., Challis, R. E. & Wedlock, D. J. 1994 A wide-bandwidth ultrasonic study of suspensions: the variation of velocity and attenuation with particle size. *J. Colloid Interface Sci.* **168**, 339–348.

Kurtze, G. & Tamm, K. 1953 Measurements of sound absorption in water and aqueous solutions of electrolytes. *Acustica* **3**, 34–48.

Lamb, H. 1945 *Hydrodynamics*. New York: Dover.

Leighton, T. G., Brown, N. R. & Richards, S. D. 2002 Effect of acoustic absorption by hydrophone and cable on a reverberation technique for measuring sound absorption coefficient of particulate suspensions. ISVR Technical Report no. 299, University of Southampton, Southampton, UK.

Moss, S. H. O. & Attenborough, K. 1996 Measurements of the narrow-band decay rates of a gas/particle suspension confined in a cylindrical tube: relationship to particle concentration. *J. Acoust. Soc. Am.* **100**, 1992–2001.

Pierce, A. D. 1994 *Acoustics: an introduction to its physical principles and applications*. New York: Acoustical Society of America.

Qian, Z. W. 1996 Fractal dimensions of sediments in nature. *Phys. Rev.* E **53**, 2304–2306.

Richards, S. D. 2002 Visco-inertial dissipation in dilute particulate suspensions. PhD thesis, University of Southampton, UK.

Richards, S. D. & Leighton, T. G. 2000 Sonar performance in turbid and bubbly environments. *J. Acoust. Soc. Am.* **108**, 2562.

Richards, S. D. & Leighton, T. G. 2001 Acoustic sensor performance in coastal environments: suspended sediments and microbubbles. In *Acoustical oceanography* (ed. T. G. Leighton, G. J. Heald, H. D. Griffiths & D. Griffiths). *Proc. Institute of Acoustics*, vol. 23, pp. 399–406.

Richards, S. D., Heathershaw, A. D. & Thorne, P. D. 1996 The effect of suspended particulate matter on sound attenuation in turbid coastal waters. *J. Acoust. Soc. Am.* **100**, 1447–1450.

Schroeder, M. R. 1965 New method of measuring reverberation time. *J. Acoust. Soc. Am.* **37**, 409–412.

Stokes, G. G. 1851 On the effect of the internal friction of fluids on the motion of pendulums. Part II. *Trans. Camb. Phil. Soc.* **9**, 8–106.

Temkin, S. & Dobbins, R. A. 1966 Attenuation and dispersion of sound by particle-relaxation processes. *J. Acoust. Soc. Am.* **40**, 317–324.

Urick, R. J. 1948 The absorption of sound in suspensions of irregular particles. *J. Acoust. Soc. Am.* **20**, 283–289.

Wang, Q., Attenborough, K. & Woodhead, S. 2000 Particle irregularity and aggregation effects in airborne suspensions at audio and low ultrasonic frequencies. *J. Sound Vib.* **236**, 781–800.